*Int. J. Heat Mass Transfer.* Vol. 30, No. 12, pp. 2617–2625, 1987
Printed in Great Britain

0017–9310/87 $3.00 + 0.00
Pergamon Journals Ltd.

# Effect of seed droplet evaporation on electrical conductivity and temperature of combustion plasmas

N. S. DIXIT, N. VENKATRAMANI and V. K. ROHATGI
Plasma Physics Division, Bhabha Atomic Research Centre, Trombay, Bombay 400 085, India

(*Received* 17 *October* 1985 *and in final form* 15 *January* 1987)

**Abstract**—The electrical conductivity of the working medium of a combustion driven MHD generator is increased by introducing a low-ionization potential additive (seed). This seed is in the form of a fine spray of an aqueous solution of $K_2CO_3$ by an atomizer. However, the electrical conductivity depends strongly on the evaporation process and the evaporation in turn depends on the size of droplets. In this paper, the effect of seed droplet size on evaporation (and hence on electrical conductivity and plasma temperature) have been analysed by formulating a single step finite rate evaporation model. Experiments were conducted to measure plasma temperature and conductivity on a potassium seeded combustion plasma system by introducing seed droplets of different sizes. The measured and the predicted values have been compared to substantiate the model.

## 1. INTRODUCTION

IN AN OPEN cycle MHD generator, to increase the electrical conductivity of the working medium, a low ionization potential additive, called seed, is added. Normally, potassium in the form of a fine spray of an aqueous solution of $K_2CO_3$ is added by an atomizer [1]. Since the potassium in the solution takes a finite time before getting ionized, the electrical conductivity of the combustion plasma strongly depends on the evaporation process. Thus, it is essential to analyse this phenomenon since the MHD power generated is directly proportional to the electrical conductivity of the working medium [2]. In this paper, with the help of the single step model developed, the effect of droplet size on the evaporation process is analysed. Experiments were conducted on combustion plasma ($LPG + O_2 +$ seed) system to measure electrical conductivity and temperature by introducing seed droplets of different size. The measured temperatures and conductivity have been compared with the predicted values.

## 2. FORMULATION OF THE MODEL

### 2.1. *Mechanism of seed evaporation*

The droplets of seed introduced into the combustion products (C.P.) by an atomizer undergo the following processes before part of the potassium atoms are ionized:

(a) heating of aqueous seed solution from ambient temperature to the boiling point;
(b) evaporation of water leading to a saturated solution of $K_2CO_3$;
(c) crystallization of potassium carbonate;
(d) heating of crystals of $K_2CO_3$;
(e) melting of $K_2CO_3$;
(f) heating of molten $K_2CO_3$;
(g) evaporation and dissociation of $K_2CO_3$; and
(h) ionization of potassium atoms.

The study of evaporation of a single droplet using the multistep (steps (a)–(h) above) evaporation model was done by Golovin and Perochin [3]. This was extended by Sharma *et al.* [4] for a droplet distribution as occurs in a spray. In these models, the steps described above (steps (a)–(h)) occur one at a time on each of the droplets.

In this paper, a simplified single step model has been developed. In this model all the droplets are assumed to have the Sauter mean (s.m.) diameter of the distribution calculated using the Nukiyama–Tanasawa relation [5] and travel with the same velocity of gas.

Evaporation occurs over a thin shell of the droplet which goes through all the processes described earlier. The rest of the droplet is at the initial temperature. Further, the droplets are assumed to be spherical and the spray to be dilute so that the collisions between the droplets are not important and hence no discontinuous processes like coalescing, breaking up of droplets takes place.

### 2.2. *Mathematical modelling of droplet evaporation*

When the seed solution is introduced by an atomizer, the diameter of the droplets is governed by the flow rates of solution, atomizing gas, in addition to viscosity, surface tension and density of the solution [5]. The diameter, which is the Sauter mean diameter, is calculated using the Nukiyama–Tanasawa relation.

Consider a unit volume of gas containing $n_s$ droplets

## NOMENCLATURE

$A$ area of cross-section [$m^2$]
$B$ transfer number
$C_g$ specific heat of gas [$J\,kg^{-1}\,K^{-1}$]
$\bar{C}_g$ specific heat of gas at mean film temperature [$J\,kg^{-1}\,K^{-1}$]
$d_0$ initial diameter of droplet [m]
$e_s$ evaporation rate of seed solution per unit volume of gas [$kg\,m^{-3}$]
$f$ fraction evaporated
$G_g^0$ mass flow rate of the gas [kg]
$G_s$ mass flow rate of the solution [kg]
$h$ plasma enthalpy [$J\,kg^{-1}$]
$h_s$ enthalpy of droplets [$J\,kg^{-1}$]
$h$ thermal conductivity at mean film temperature [$W\,m^{-1}\,K^{-1}$]
$L$ enthalpy per unit mass required to heat up the droplet from the ambient temperature to the boiling point [$J\,kg^{-1}$]
$n_s$ droplet number density [$m^{-3}$]
$q_s$ heat loss to the droplet per unit volume [$W\,m^{-3}$]
$q_w$ heat loss to the walls per unit volume of plasma [$W\,m^{-3}$]
$r$ radius of droplet [m]
$T_g$ temperature of plasma [K]
$\bar{T}_s$ mean temperature of the shell of the droplet [K]
$u$ gas velocity [$m\,s^{-1}$]
$u_s$ droplet velocity [$m\,s^{-1}$].

Greek symbols
$\rho$ gas density [$kg\,m^{-3}$]
$\rho_s$ droplet density [$kg\,m^{-3}$]
$\sigma$ plasma electrical conductivity [$S\,m^{-1}$].

of radius $r$. The total evaporation rate per unit volume $e_s$ is given by [6]

$$e_s = \frac{n_s 4\pi r^2 h^0}{C_g} \ln(1+B). \tag{1}$$

If $\bar{k}$ is the thermal conductivity at mean film temperature, then, it can be shown, for the present case, that

$$h^0 = \frac{\bar{k}}{r}.$$

The transfer number $B$ is given by

$$B = \bar{C}_g(T_g - \bar{T}_s)/L.$$

The radius $r$ can be expressed in terms of the initial droplet diameter $d_0$ and the fraction $f$ by

$$r = (1-f)^{1/3} d_0/2.$$

The number of droplets $n_s$ can also be represented in terms of the seed solution flow rate $G_s^0$, density $\rho_s$ and the initial velocity of the solution $u_0$ by

$$G_s^0 = n_s(\tfrac{1}{6}\pi d_0^3 \rho_s) u_0 A.$$

Substituting these values in the equation for $e_s$, we obtain

$$e_s = \frac{12 G_s^0}{\rho_s d_0^2 u_0 A}(1-f)^{1/3}\left[\frac{\bar{k}}{\bar{C}_g}\ln\left\{1+\frac{C_g(T_g-\bar{T}_s)}{L}\right\}\right]. \tag{2}$$

Since the evaporation rate can also be given by

$$e_s = \frac{\mathrm{d}}{\mathrm{d}t}\left(h_s \frac{\pi}{6} d_0^3 \rho_s\right)$$

the equation can be solved to give $f$ as an explicit function of time $t$, with the initial conditions, that, $f = 0$ at $t = 0$

$$1-(1-f)^{1/3} = \frac{2}{\rho_s}\left[\frac{\bar{k}}{\bar{C}_g}\ln\left\{1+\frac{C_g(T_g-\bar{T}_s)}{L}\right\}\right]\frac{4t}{d_0^2}. \tag{3}$$

A plot of $f$ against $4t/d_0^2$ is shown in Fig. 1 in which a comparison between multistep modelling [4] and single step modelling is made. It is seen that for a given droplet diameter ($d_0$), the single step modelling, compared to the multistep model, slightly overestimates the evaporation time ($\sim 15\%$).

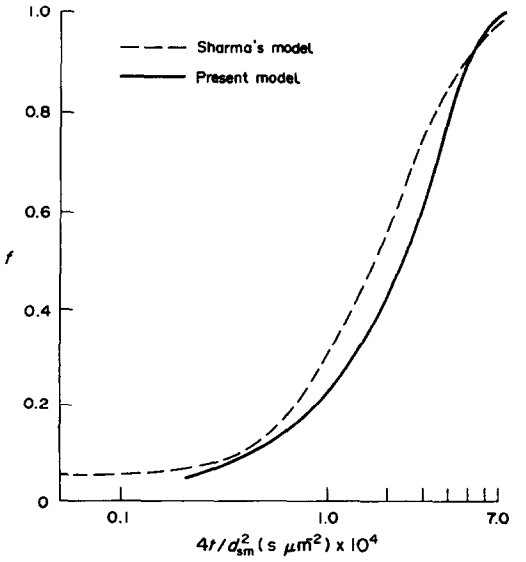


FIG. 1. Fraction evaporated as computed by multistep and single step modelling.

2.3. *Flow modelling*

The flow in a duct, as in the present case, is in general a three-dimensional phenomenon and an exact analysis is extremely difficult. However, when there is a dominant flow direction, a one-dimensional or quasi-one-dimensional analysis can be made. Thus, the present problem of flow of evaporating seed droplet in hot combustion products can be treated as quasi-one-dimensional two phase flow of an inviscid gas (no friction) with heat transfer to the walls.

The conservation equations of mass, momentum and energy with implicit approximations for the two phase flow are given in ref. [7]. Further, in the present problem, the process is near atmospheric and droplets and the gas move with the same velocity. Therefore, the momentum conservation equation need not be evaluated. The basic equations are thus:

*conservation of mass*

$$\text{(i) gas:} \quad \frac{\mathrm{d}}{\mathrm{d}x}(\rho u) = e_s \tag{4}$$

$$\text{(ii) droplet:} \quad \frac{\mathrm{d}}{\mathrm{d}x}(\rho_s u_s) = -e_s \tag{5}$$

*conservation of energy*

$$\text{(i) gas:} \quad \frac{\mathrm{d}}{\mathrm{d}x}\left\{\rho u\left(h+\frac{u^2}{2}\right)\right\} = -q_w - q_s \tag{6}$$

$$\text{(ii) droplet:} \quad \frac{\mathrm{d}}{\mathrm{d}x}(\rho_s u_s h_s) = q_s. \tag{7}$$

The equation can in principle be solved to yield the unknowns $\rho$, $\rho_s$, $u$, $u_s$, $h$ if $h_s$ and $h(\rho)$ are available.

In a practical problem, the important variables are the temperature $T$, and the fraction '$f$' of the seed solution that is evaporated. Thus, equations (4)–(7) can be simplified to yield explicit expressions for $T$ and $f$.

Using the mass conservation equation, we obtain

$$\frac{\mathrm{d}}{\mathrm{d}x}(G_s) = \frac{\mathrm{d}}{\mathrm{d}x}\{(1-f)G_s^0\} = -e_s A$$

or

$$\frac{\mathrm{d}f}{\mathrm{d}x} = \frac{e_s A}{G_s^0}. \tag{8}$$

Equations (4) and (6) yield

$$\frac{\mathrm{d}}{\mathrm{d}x}(h+u^2/2) = -\frac{q_w+q_s+e_s(h+u^2/2)}{\rho u} = -\frac{q_w+q_s+e_s(h+u^2/2)}{\frac{1}{A}(G_g^0+fG_s^0)}. \tag{9}$$

In the model, $T_s$ remains constant, $h_s$ remains constant, solving equation (7) we obtain

$$q_s = -h_s\rho_s.$$

Thus in equation (9), neglecting $u^2/2$ being extremely small in the present case in comparison with $h$ and substituting for $q_s$ and writing $C_g = \mathrm{d}h/\mathrm{d}T$, we obtain

$$\frac{\mathrm{d}T}{\mathrm{d}x} = \frac{q_w+e_s(h-h_s)}{C_g}\frac{A}{G_g^0+fG_s^0}. \tag{10}$$

Thus, making use of equations (2), (8) and (10), one can estimate the evaporation rate of a droplet, fraction of the droplet evaporated and fall of temperature along the length of the channel. The fraction of seed evaporated, as estimated above, can in turn be used to determine the plasma electrical conductivity which can be compared with that of the experimental value.

## 3. EXPERIMENT

The measurements were carried out in an LPG–$O_2$ combustion rig. The experimental set up consists of a combustor, mixing chamber, test section, an extension duct, spray cooling chamber, and exhaust as shown in Fig. 2(a). The details of the relevant parts are given below.

*Combustor*: The combustor is completely water cooled and incorporates the seeding nozzle in the central part. The oxidizer comes from the peripheral 8 holes of 1.5 mm diameter at an inclination of 30° to the axis whereas the fuel comes through 4 holes of 1.0 mm diameter parallel to the axis. The seed solution is introduced through an s.s. tube of i.d. 1 mm and o.d. 1.5 mm. It is positioned in the central plug with a hole of 2.5 mm diameter. The atomizing gas ($O_2$) comes through the tapered annular space as shown in Fig. 2(b).

The combustor operates with a large back radiation from the mixing chamber walls facing the combustor. A few design alternatives were made on the combustor, seeding nozzles, etc. Of these, the present design performed well with a stable flame, without overheating or clogging of the seed solution. It is also possible to retract completely the seed nozzle for cleaning and to reintroduce at the time of measurements.

*Mixing chamber*: It is a cylindrical double walled chamber, internally lined with $ZrO_2$. It has an internal cross-section diameter of 50 mm with two ports, for introducing pilot flame and flame detector.

*Test section*: It is a double walled chamber with an internal c.s. after $Al_2O_3$ lining, of 50 mm × 50 mm of length 150 mm. It has two diagnostic ports on opposite walls. These diagnostic ports were used for measuring the plasma temperature by the spectroscopic line reversal technique and the electrical conductivity by radio-frequency 'Q' probe [8].

The seed solution is stored in an s.s. tank with needle valve and flow meter for monitoring the seed-solution flow. The tank can be pressurized to 1.5 atm by nitrogen to ensure uniform flow of the solution.

*Seed atomization*: Experiments were carried out to measure the seed droplet sizes, under ambient temperature conditions [5]. For the given geometry of the combustor nozzle assembly, seed flow rate and oxygen

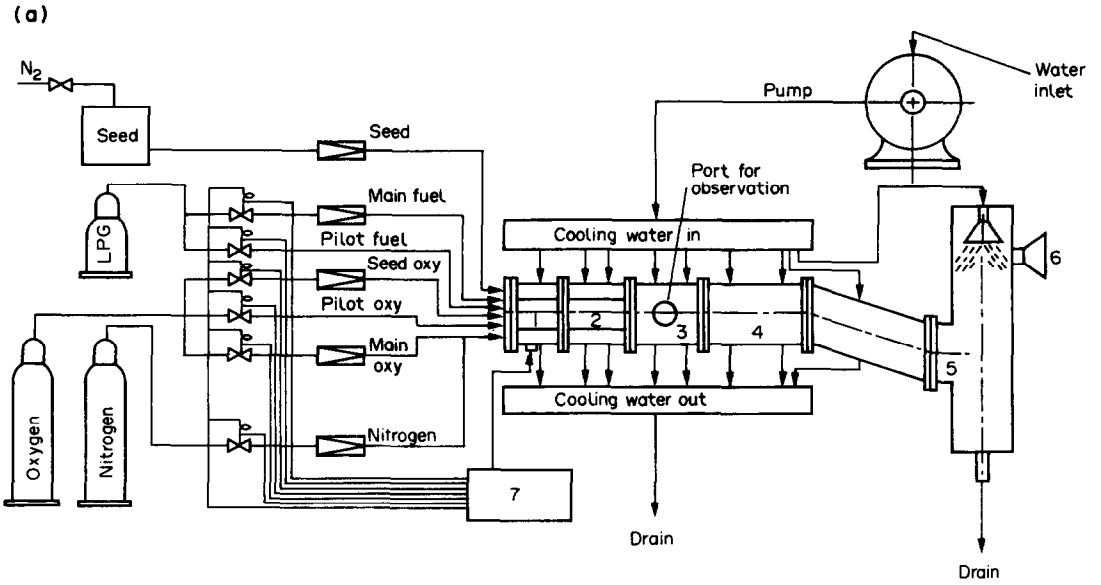


FIG. 2(a). Schematic of the experimental rig: 1, combustor; 2, mixing chamber; 3, test section; 4, connecting channel; 5, spray cooling chamber; 6, exhaust fan; 7, control console.

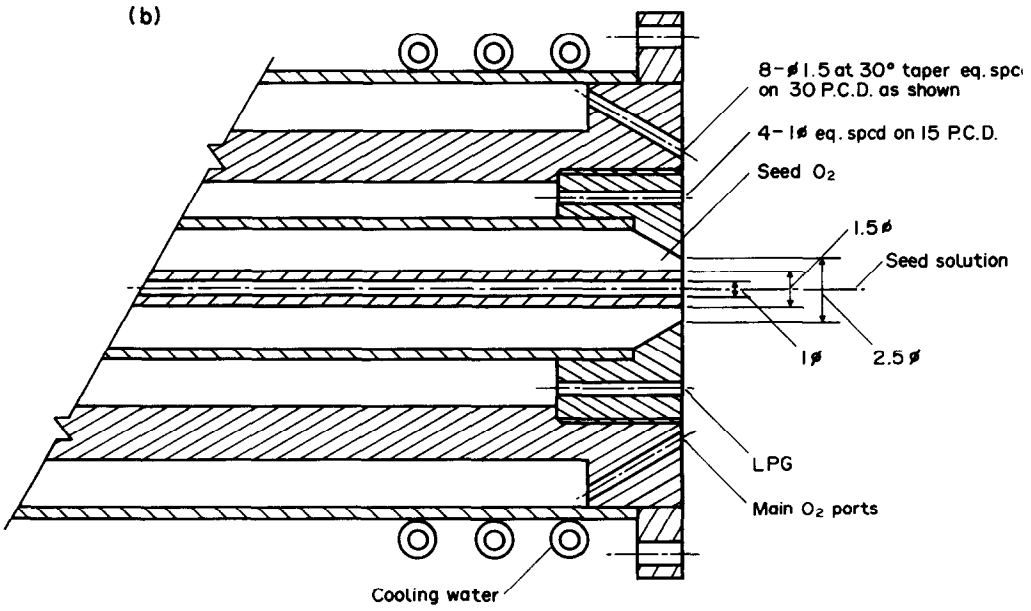


FIG. 2(b). Details of burner.

flow rates were measured. The specific nozzles used are shown in the figures. The drop size was measured by using impingement of the droplets on glass slides which were vacuum coated with a thin film of aluminium. The slides were held at a distance of 20 cm from the nozzle. Potassium hydroxide solution was used which etched away the aluminium coating. To stop further etching with time, the slides were immediately washed with water after exposure. Thus a permanent record of droplet size was obtained and actual measurements were made with an optical microscope by counting the number and sizes of droplets. Typical histograms are given in Fig. 3. The histograms were smoothed out to give droplet size frequency curves.

Nukiyama–Tanasawa also proposed that the droplet sizes could be correlated by the empirical distribution function given by

$$\frac{dn}{dx} = bx^m e^{-cx^\phi}.$$

For high gas velocities (150–200 m $s^{-1}$) and large volumetric ratio of gas–liquid ($\sim$2000), $m = 2$

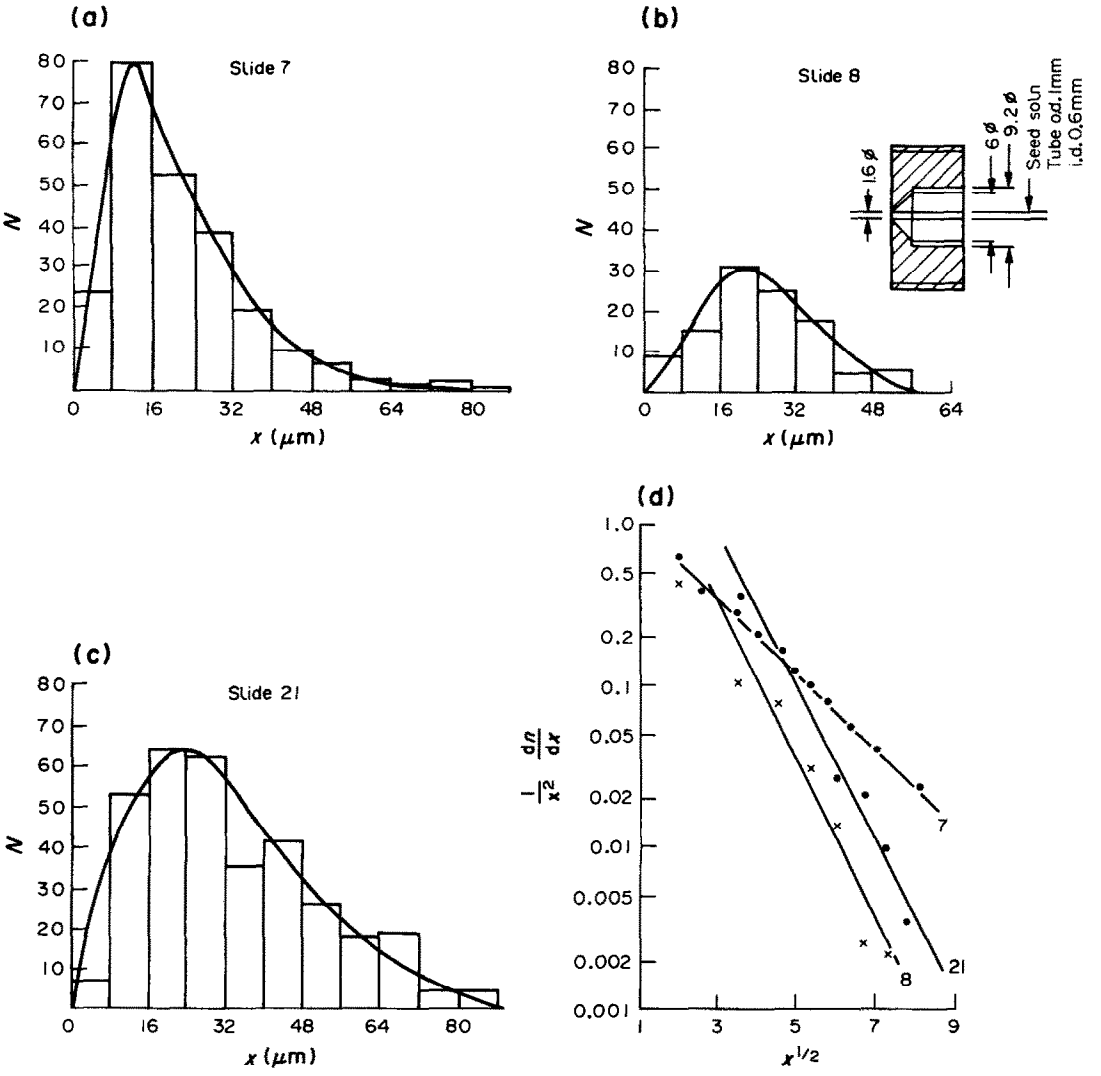


FIG. 3. Histograms of droplet distribution.

whereas $\delta$ can take a variety of values 1/2, 1/3, 1/4, etc. The above equation can be written as

$$\log\left\{\frac{1}{x^2}\frac{dn}{dx}\right\} = \log b - cx^{\delta}.$$

Various values of $\delta$ were tried and it was found that $\delta = 1/2$ gives a straight line. The plots are given in Fig. 3(d).

The calculated and measured Sauter mean diameters were compared and s.m. diameter in the range 30–60 $\mu$m, the maximum difference between calculated and measured values was 15%. From this it was concluded that the Nukiyama–Tanasawa equation can predict the droplet sizes for the given geometry, with relevant physical parameters of flow and solution.

The actual dimensions of the seed spray nozzle are given in Fig. 2(b). The slightly changed dimensions were chosen so that at the high temperature environment the seed solution does not crystallize in the tube itself at low flow rates.

## 4. RESULTS AND DISCUSSIONS

The equations of Section 2.3 have been solved for 20 kW thermal input and the results are compared with those of measured values. Figure 4 shows the variation of temperature along the length of the section for a mean droplet diameter of 50 $\mu$m. The drop in temperature occurs due to heat loss to the coolant through walls due to the evaporation of the seed solution. The fraction of the seed evaporated along the length of the section for a typical flow rate of seed, corresponding to 1% potassium in C.P., is shown in Fig. 4. From the curve, we see that the larger the diameter, the amount of seed vaporized is less. For a diameter of 70 $\mu$m, the amount of seed evaporated at a distance of 20 cm from the burner is slightly more

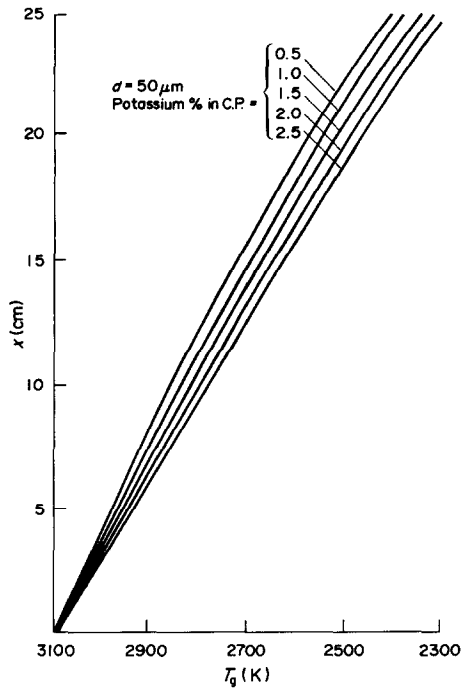


FIG. 4. Variation of plasma temperature along the length of the channel.

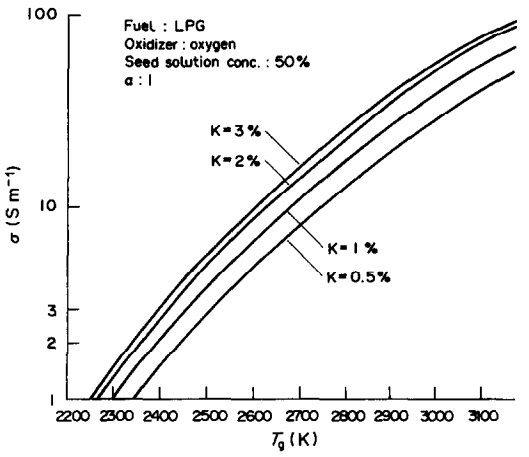


FIG. 6. Estimated plasma electrical conductivity as a function of temperature for different seed percentage in C.P. assuming instantaneous evaporation.

than 50%. In other words, almost 50% of potassium is still in the condensed phase and does not contribute to the electrical conductivity. Taking the temperature of the plasma and the fraction of seed droplet evaporated, from Figs. 4 and 5, the actual conductivity of the plasma is determined using Fig. 6. The conductivity along the length of the channel is plotted in Fig. 7.

For comparing the effect of partial evaporation on conductivity, with that of complete evaporation, the calculated values of conductivity for a diameter of 50 μm for 1% potassium, are plotted in Fig. 8. It can be clearly seen that as one proceeds downstream, more and more seed evaporates and both the curves become nearly identical (at a distance of 20 cm from the combustor).

The measuring point is located at 19.5 cm from the inlet. So, the calculated values of conductivity at 19.5 cm for different diameters are shown in Fig. 9. The general pattern of the curves can be explained as follows: when the diameter is small, the evaporation is complete before the measuring point; the addition of extra seed, above 1% leads to a drop in temperature resulting in reduced conductivity. On the other hand, with a large diameter, seed evaporation is less and hence the increase in the quantity of seed leads to an increase in conductivity. However, for in between these extreme diameters, there are optimum values of

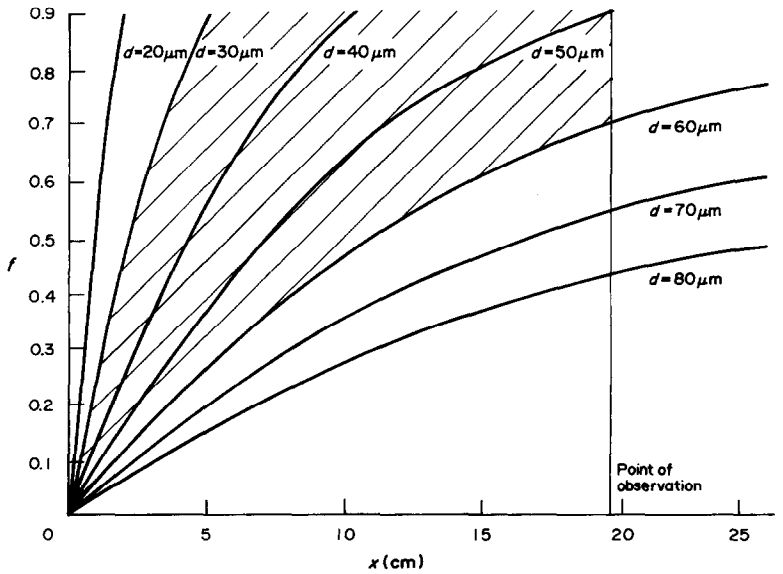


FIG. 5. Fraction $f$ evaporated along the length of the channel for different droplet diameters.

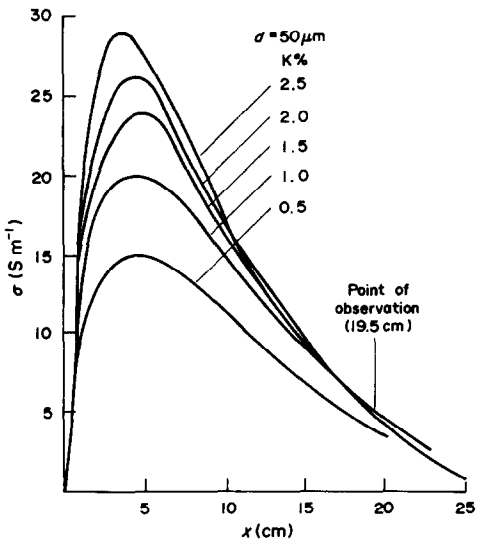


FIG. 7. Variation of plasma electrical conductivity along the length of the channel.

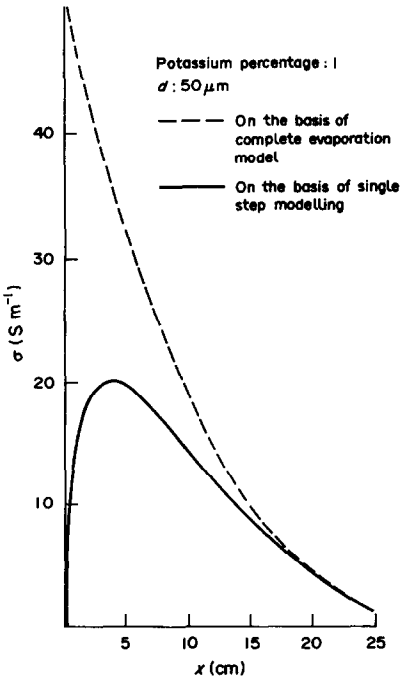


FIG. 8. Comparison of plasma electrical conductivity estimated by single step and complete evaporation model.

seeding when the conductivity is maximum, at the measuring point. Also indicated on the same figure are the experimental values. We see that for a mean droplet diameter of around 40 $\mu$m, as calculated for the given geometry, the estimated values of conductivity maxima occurs around 1.4–1.6% corresponding to complete evaporation, leading to a conductivity of around 4.25 S m$^{-1}$. The experimental data agrees reasonably with the calculated conductivity, the maxima occurring around 1.7–1.8% of potassium,

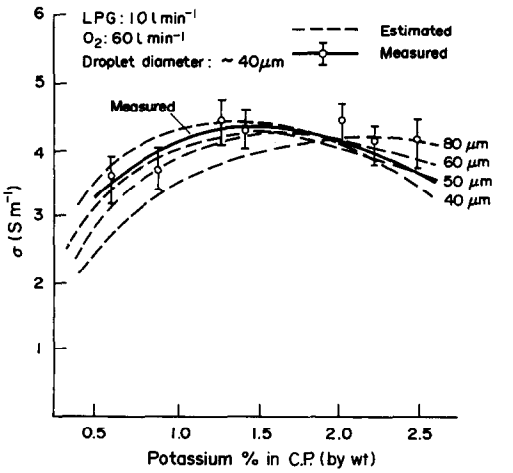


FIG. 9. Plasma electrical conductivity for different diameters at 19.5 cm from the combustor.

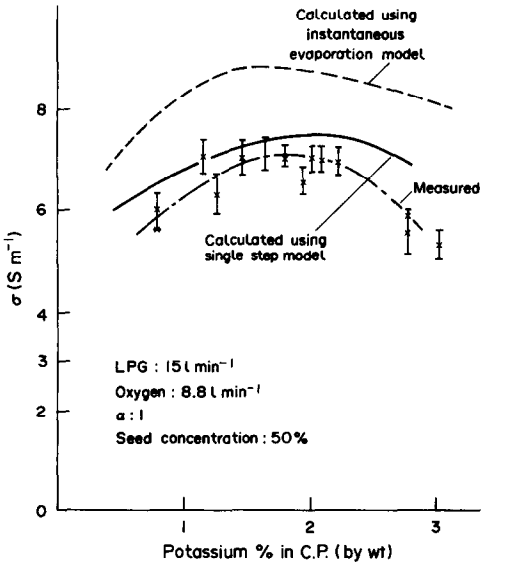


FIG. 10. Comparison of estimated and measured plasma electrical conductivity.

the value of electrical conductivity (measured) being 4.5 S m$^{-1}$.

The validity of the model is further substantiated in Fig. 10 in which measured conductivity, estimated conductivity using the instantaneous evaporation model [10] and single step model are plotted. We see that the measured conductivity values are much less than the estimated ones when compared with the instantaneous evaporation model whereas the same agree well with the estimated ones using the single step finite rate evaporation model.

The calculated temperatures at the measuring point using the single step model and the measured ones are plotted in Fig. 11. We see there is a good agreement at the lower seed percentage, whereas with increased seeding they are less than the calculated ones ($\sim$ 1.2 at 2% potassium in C.P.). This is because, with increased seeding, the amount of seed in the gas phase increases

leading to strong self-absorption in the boundary layers. This self-absorption increases the error in the measurement by a little more than 30 K. Such observations are also made by other workers [9].

It is also seen that as the seeding increases from 0–2%, there is around a 200 K drop in the plasma temperature. This is due to the fact that an addition of 1 kg of potassium in combustion product involves an addition of 1.77 kg of $K_2CO_3$ and hence 3.54 kg of 50% aqueous solution. Therefore, the large drop in temperature arises due to the addition of the compound along with water in the seed solution. A comparison with the corresponding temperature drop in theoretically calculated flame temperature including the thermal losses in the system [8] shows full confirmity.

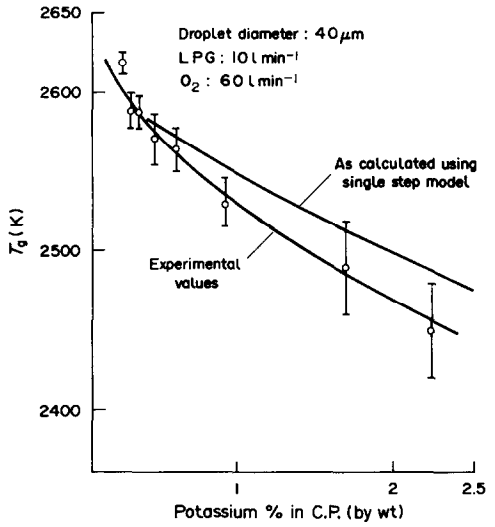


FIG. 11. Comparison of measured plasma temperature with the estimated ones using the single step model.

## 5. CONCLUSIONS

Electrical conductivity of a combustion plasma seeded with potassium in the form of an aqueous solution of $K_2CO_3$ was measured for different droplet diameters. Measured values were found to be less than the theoretical ones, estimated based on the instantaneous evaporation model. However, the measured values matched well with the single step finite rate evaporation model. Hence, it can be concluded that the lowering of conductivity can be attributed to the partial evaporation of the finite sized seed droplets, which is an important point to be considered while designing an MHD channel, etc.

## REFERENCES

1. N. Venkatramani, R. Jayakumar, D. R. Iyer and N. S. Dixit, Experimental rig for MHD studies, Symp. on Plasma Physics and MHD, BARC, Bombay (1975).
2. G. M. Sutton and A. Sherman, *Engineering Magnetohydrodynamics*. McGraw-Hill, New York (1965).
3. A. M. Golovin and V. R. Perochin, Evaporation of a drop of solution in a high temperature medium, *High Temperature* **14**(4), 720 (1970).
4. R. Sharma, N. Venkatramani and V. K. Rohatgi, Modelling of seed droplet evaporation in combustion products, BARC Report 1020 (1979).
5. R. K. Marwah, N. S. Dixit, N. Venkatramani and V. K. Rohatgi, Distribution of droplet sizes for seed solution, BARC, PPS Internal Report (1977).
6. A. M. Kanuri, *Introduction to Combustion Phenomenon*. Gordon & Breach, New York (1975).
7. R. Sharma, A. K. Das, N. Venkatramani and V. K. Rohatgi, An appraisal of MHD generator performance with coal based fuels and aqueous seed solution, VII Int. Conf. on MHD Power Generation, Cambridge (1980).
8. N. S. Dixit, Ph.D. Thesis, Bombay University (1983).
9. Kaz Onda, Yasuo Kaga and Ken Kato, Measurement of MHD combustion gas temperature and potassium number densities in the presence of cold boundary layers, *J. Quant. Spectrosc. Radiat. Transfer* **26**, 146–156 (1981).
10. A. K. Das, Ph.D. Thesis, Bombay University (1979).

## EFFET DE L'EVAPORATION D'UN ENSEMENCEMENT DE GOUTTELETTES SUR LA CONDUCTIVITE ELECTRIQUE ET LA TEMPERATURE DES PLASMAS DE COMBUSTION

**Résumé**—La conductivité électrique d'un milieu en combustion pilotée par un générateur MHD est augmentée par l'introduction d'un additif à faible potentiel d'ionisation (semence). Cet ensemencement, sous la forme d'un aérosol de gouttelettes d'une solution aqueuse de $K_2CO_3$, est réalisé par un atomiseur. Néanmoins la conductivité électrique dépend fortement du mécanisme d'évaporation et en retour l'évaporation dépend de la taille des gouttelettes. Dans cette étude, l'effet de la taille des gouttelettes sur l'évaporation (et par suite, sur la conductivité électrique et la température du plasma) a été analysé en formulant un modèle d'échelon fini, unique, d'évaporation. Des expériences sont conduites pour mesurer la température de plasma et la conductivité d'un système de plasma en combustion et ensemencé de potassium avec des gouttelettes de différentes tailles. Les valeurs mesurées et calculées ont été comparées pour affermir le modèle.

## DER EINFLUSS DER VERDAMPFUNG VON "IMPF"-TROPFEN AUF DIE ELEKTRISCHE LEITFÄHIGKEIT UND DIE TEMPERATUR EINES VERBRENNUNGS-PLASMAS

**Zusammenfassung**—Die elektrische Leitfähigkeit des Arbeitsmediums eines durch Verbrennung getriebenen MHD-Generators wird durch Einleiten eines gering ionisierten Potential-Additivs ("Impfung") verbessert. Diese Impfung wird in Form eines feinen Sprays einer wäßrigen $K_2CO_3$-Lösung durchgeführt. Die elektrische Leitfähigkeit hängt stark von der Tropfengröße ab. In dieser Arbeit wurden die Einflüsse der Impf-Tropfengröße auf die Verdampfung (und damit auf die elektrische Leitfähigkeit und die Plasmatemperatur) durch Formulierung eines Einzelschritt-Verdampfungsmodells untersucht. Versuche wurden durchgeführt, um Plasmatemperaturen und die elektrische Leitfähigkeit eines mit Kalium geimpften Verbrennungsplasma-Systems durch Einleiten von Impf-Tropfen unterschiedlicher Größe zu messen. Um das Modell zu untermauern, wurden die gemessenen und berechneten Werte verglichen.

## ВЛИЯНИЕ ИСПАРЕНИЯ КАПЕЛЬ ИОНИЗИРУЮЩЕЙ ДОБАВКИ НА ЭЛЕКТРОПРОВОДНОСТЬ И ТЕМПЕРАТУРУ ПЛАЗМЫ ПЛАМЕНИ

**Аннотация**—Электропроводность рабочей среды в МГД плазмогенераторе увеличивается при введении добавки с низким потенциалом ионизации, представляющей собой мелкий распыл водного раствора $K_2CO_3$, вводимого распылителем. Однако, электропроводность сильно зависит от процесса испарения, который, в свою очередь, зависит от размера капель. В данной работе влияние размера капель добавки на испарение (и, следовательно, на электропроводность и температуру плазмы) проанализировано с помощью предложенной одностадийной модели испарения с конечной скоростью. Проведены эксперименты по измерению температуры плазмы и электропроводности плазменного факела при введении капель калия различных размеров. Для обоснования предложенной модели проведено сравнение результатов измерения и расчетных данных.